

Controlling Polymerization Initiator Concentration in Mesoporous Silica

Thin Films – Supporting Information

Fabio Krohm¹, Haiko Didzoleit², Marcus Schulze³, Christian Dietz³, Robert W. Stark³, Christian Hess⁴,

Bernd Stühn², Annette Brunsen^{1}*

¹Ernst-Berl Institute for Chemical Engineering and Macromolecular Science, Technische Universität
Darmstadt, Alarich-Weiss-Str. 4, D-64287 Darmstadt, Germany

²Institute of Condensed Matter Physics, Technische Universität Darmstadt, Hochschulstraße 8, D-64289
Darmstadt, Germany

³ Center of Smart Interfaces and Department of Material and Earth-Sciences, Physics of Surfaces,
Technische Universität Darmstadt, Alarich-Weiss-Str. 10, 64287 Darmstadt, Germany

⁴ Eduard Zintl Institute for Inorganic and Physical Chemistry, Technische Universität Darmstadt,
Alarich-Weiss-Str. 8, D-64287 Darmstadt, Germany

*Corresponding author: brunsen@cellulose.tu-darmstadt.de

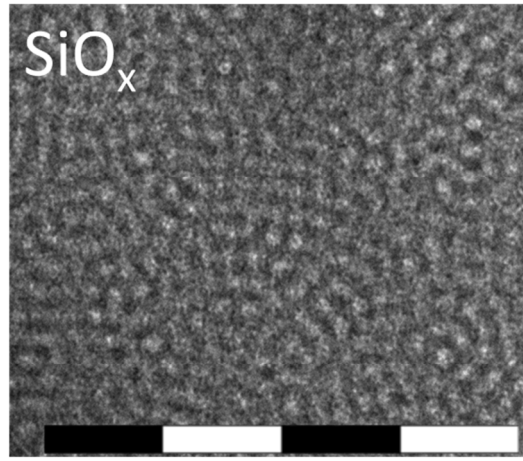


Figure S1. TEM images and porosity determined from the refractive index measured by ellipsometry using the effective medium approximation as described in the literature¹ for mesoporous silica heated to 350°C. The scalebar corresponds to 200 nm.

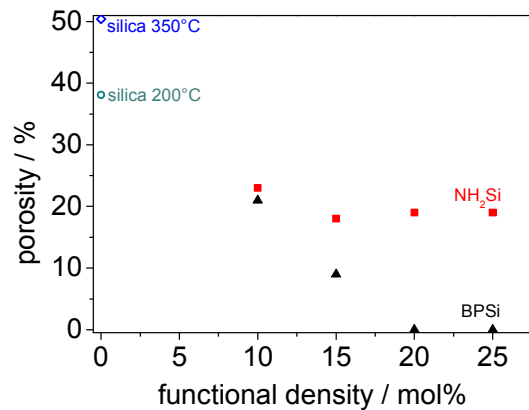


Figure S2. Film porosity as determined by effective medium theory based on the refractive index measured by ellipsometry and corresponding to Figure 2. Porosity was determined based on the refractive index of air ($n = 1$), the refractive index of silica ($n = 1.458$), and the measured refractive index of the mesoporous film by using the effective medium approximation as described in previously.¹

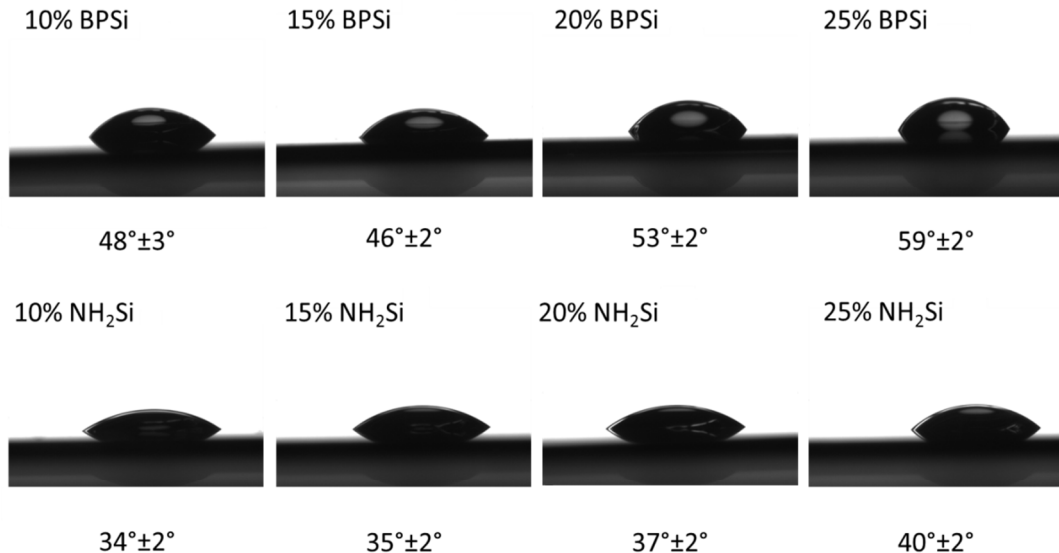


Figure S3. Sessile drop measurements. Static contact angles recorded for mesoporous thin films with increasing BPSilane (BPSi) and APTES concentration (NH₂Si) and a drop volume of 4 µL. A slightly increasing contact angle with increasing organic function is observed as expected due to the increasing amount of more hydrophobic organic compound as compared to pure mesoporous silica (contact angle < 20°). The error is based on 5 different measurement positions on the same substrate.

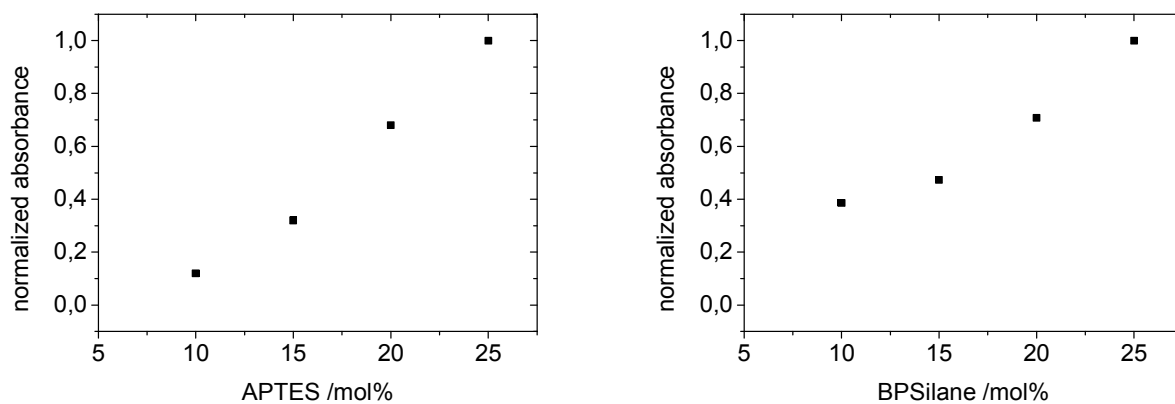


Figure S4. Overview about the normalized IR N-H bending at 1542 cm⁻¹ at pH 3 and the normalized IR C=O vibration at 1650 cm⁻¹ with increasing BPSilane ratio as extracted from Figure 6b and 6c.

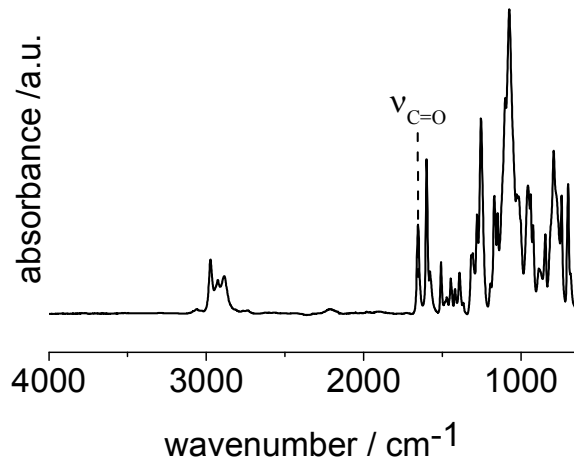


Figure S5. IR-spectrum of BPSilane as comparison to Figure 6. The C=O band is detected at 1658 cm^{-1} for pure BPSilane whereas the signal shifts to 1650 cm^{-1} for BPSi films (Figure 5). Similar shifts of C=O signals were discussed in the literature e.g. for poly(lauryl methacrylate) polymers, and attributed to interaction of the C=O function with the surface silanol groups of silica.²

Table S1. XPS-Results for all NH_2Si films corresponding to Figure 8.

Sample	C at%	O at%	N at%	Si at%	F at%	Na at%	Cl at%	xN:1Si	xF:1Si	xF:1N	%N modified with TFAA
10% NH_2Si	33.9	43.5	1.7	19.6	-	1.3	-	0.09	-	-	-
10% $\text{NH}_2\text{Si} + \text{TFAA}$	30.9	44.4	1.7	21.1	1.0	0.9	-	-	0.05	0.60	21
15% NH_2Si	36.5	42.5	2.7	17.2	-	1.0	-	0.15	-	-	-
15% $\text{NH}_2\text{Si} + \text{TFAA}$	34.6	41.5	2.1	19.5	1.3	0.9	-	-	0.07	0.62	20
25% NH_2Si	39.6	39.6	3.5	16.0	-	1.2	-	0.23	-	-	-
25% $\text{NH}_2\text{Si} + \text{TFAA}$	40.2	37.3	2.6	18.4	1.5	-	-	-	0.08	0.58	23

Analyzing the carbon content the C1s signal was fitted as summarized in Table S1b. The detected ratios of C-C : C-O : O-C=O are similar to the ones reported for an APTES-postgrafted SBA-15 silica bulk material.³

Table S1b: Results from the fit analysis of the C1s signal.

Sample	C-C		C-O		O-C=O	
	pos [eV]	area%	pos [eV]	area%	pos [eV]	area%
	284.9		286.5		288.7	
10% NH ₂ Si	284.9	65.3	286.5	29.3	288.7	5.4
15% NH ₂ Si	284.9	71.5	286.5	24.1	288.7	4.4
25% NH ₂ Si	284.9	72.6	286.5	21.6	288.7	5.7

Analyzing the C-C content per silica the XPS results indicate a higher carbon content as expected due to the introduction of APTES (3 C-C per N). One possible reason is the introduction of carbon due to unreacted or not completely condensed silica precursors TEOS and APTES. This leaves unreacted ethoxy functions which is reflected as well in the the C-O signal. Comparing the C-O ration per Si with the excess of C-C it becomes clear that ~50% of the unreacted C-C might be due to unreacted ethoxy groups resulting in ~ 1 unreacted ethoxy group per 2 Si. The same amount of C-C detected is most probably due to contamination.

Table S2. Pore diameter and interpore distance as determined by TEM.

sample	pore diameter / nm	interpore distance larger distance /nm	interpore distance smaller distance /nm
10 % NH₂Si	5.9 (± 0.8)	3.9 (± 0.7)	1.6 (± 0.5)
15 % NH₂Si	7.3 (± 0.8)	2.8 (± 0.9)	2.2 (± 0.5)
20 % NH₂Si	7.8 (± 1.1)	2.5 (± 1.3)	3.0 (± 0.9)
25 % NH₂Si	8.9 (± 0.8)	2.3 (± 1.1)	2.1 (± 0.6)
10 % BPSi	5.9 (± 0.6)	-	2.3 (± 0.8)

Table S3. Refractive index and Porosity corresponding to Figure 2.

Refractive index	Porosity /%	Sample
1.349	23	NH₂Si 10%
1.372	18	NH₂Si 15%
1.368	19	NH₂Si 20%
1.369	19	NH₂Si 25%
1.359	21	BPSi 10%
1.416	9	BPSi 15%
1.462	0	BPSi 20%
1.488	0	BPSi 25%

To determine the porosity out of refractive indices the Brüggemann effective medium approximation was used. The relation between every volume fraction inside mesoporous silica and its dielectric constant can be expressed as:

$$(p - V_p) \left[\frac{\epsilon_{\text{air}} - \epsilon_s}{\epsilon_{\text{air}} + 2\epsilon_s} \right] + (V_p) \left[\frac{\epsilon_p - \epsilon_s}{\epsilon_p + 2\epsilon_s} \right] + (1 - p) \left[\frac{\epsilon_{\text{Si}} - \epsilon_s}{\epsilon_{\text{Si}} + 2\epsilon_s} \right] = 0$$

p , V_p , ϵ_{air} , ϵ_s , ϵ_{Si} , ϵ_p correspond to the layer porosity, the polymer volume fraction, and the dielectric constants of air, the measured sample, the silica, and polymer respectively. In case mesoporous NH₂Si and BPSi without polymer the term V_p equals zero. To obtain reliable values every ellipsometric

measurement needs to run at a relative humidity below 20 %. Otherwise adsorbed air moisture is too high which consequently falsifies measurement results. The refractive index of pure SiO₂ was considered to be 1.45.

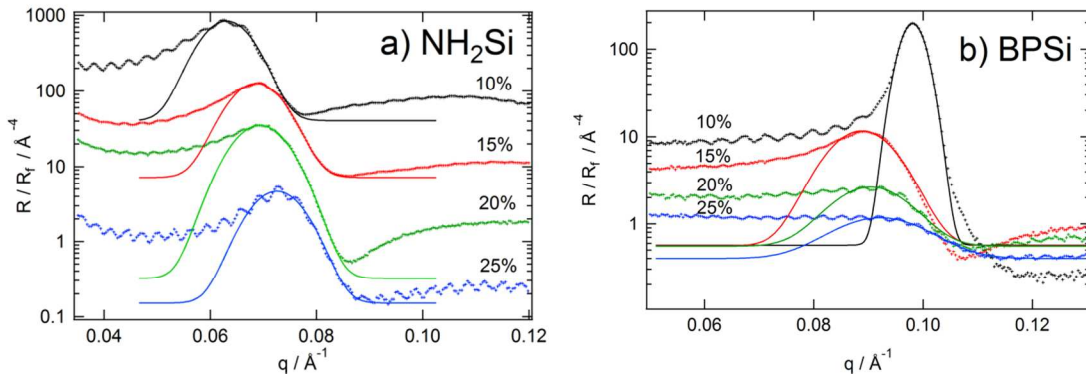


Figure S6: Reflectivity profiles have been normalized to the Fresnel reflectivity for the amino- (A) and benzophenon (B) containing silica networks. Curves have been shifted vertically for clarity. The resulting peaks are fitted with a Gaussian in order to obtain their integral intensity.

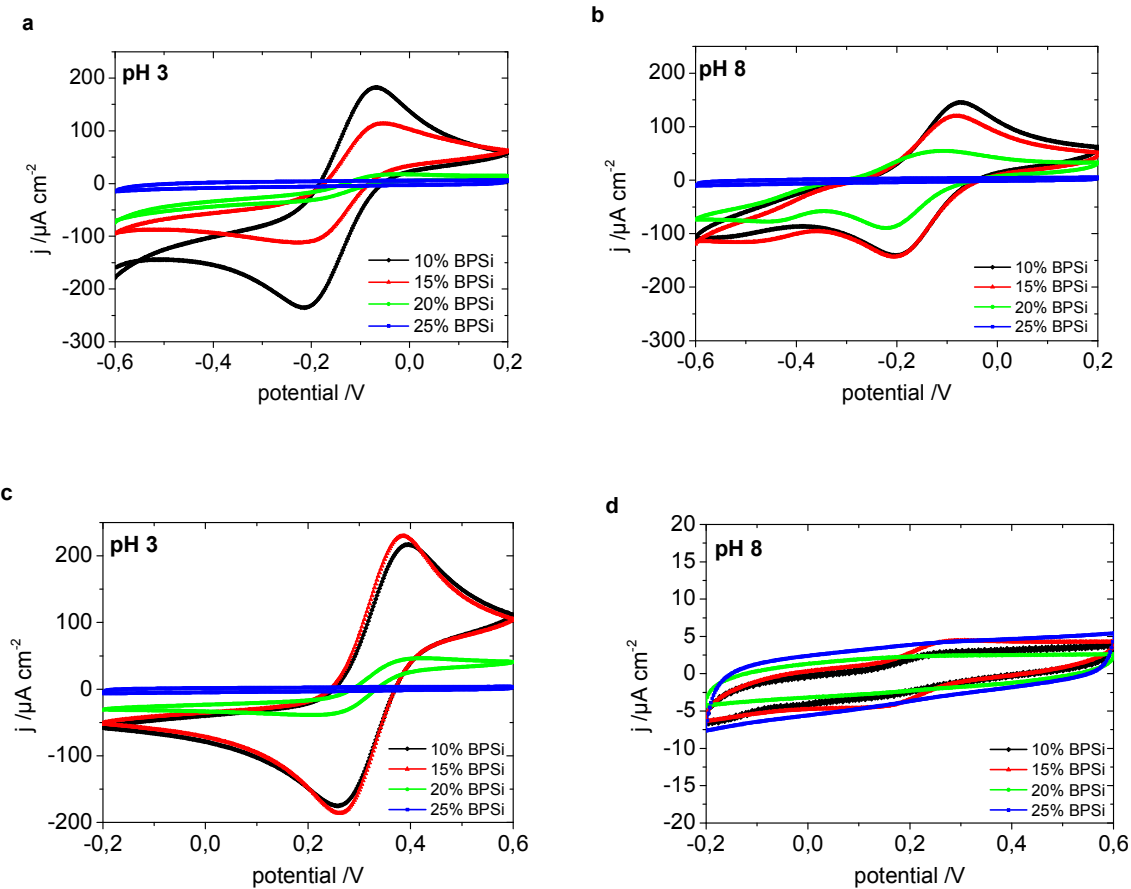


Figure S7. Cyclic voltammograms for BPSi mesoporous thin films with redox probe molecule $\text{Ru}(\text{NH}_3)_6^{3+}$ at $\text{pH} \leq 3$ (a) and $\text{pH} \geq 8$ (b) and the redox probe molecule $\text{Fe}(\text{CN}_6)^{3-}$ at $\text{pH} \leq 3$ (c) and $\text{pH} \geq 8$ (d). The BPSilane ratio of 10 mol % is shown in black, 15 mol % in red, 20 mol % in green, and 25 mol % in blue

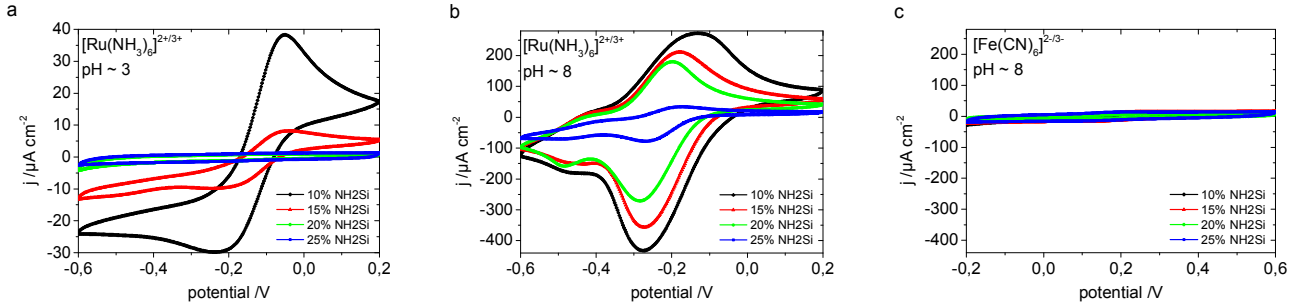
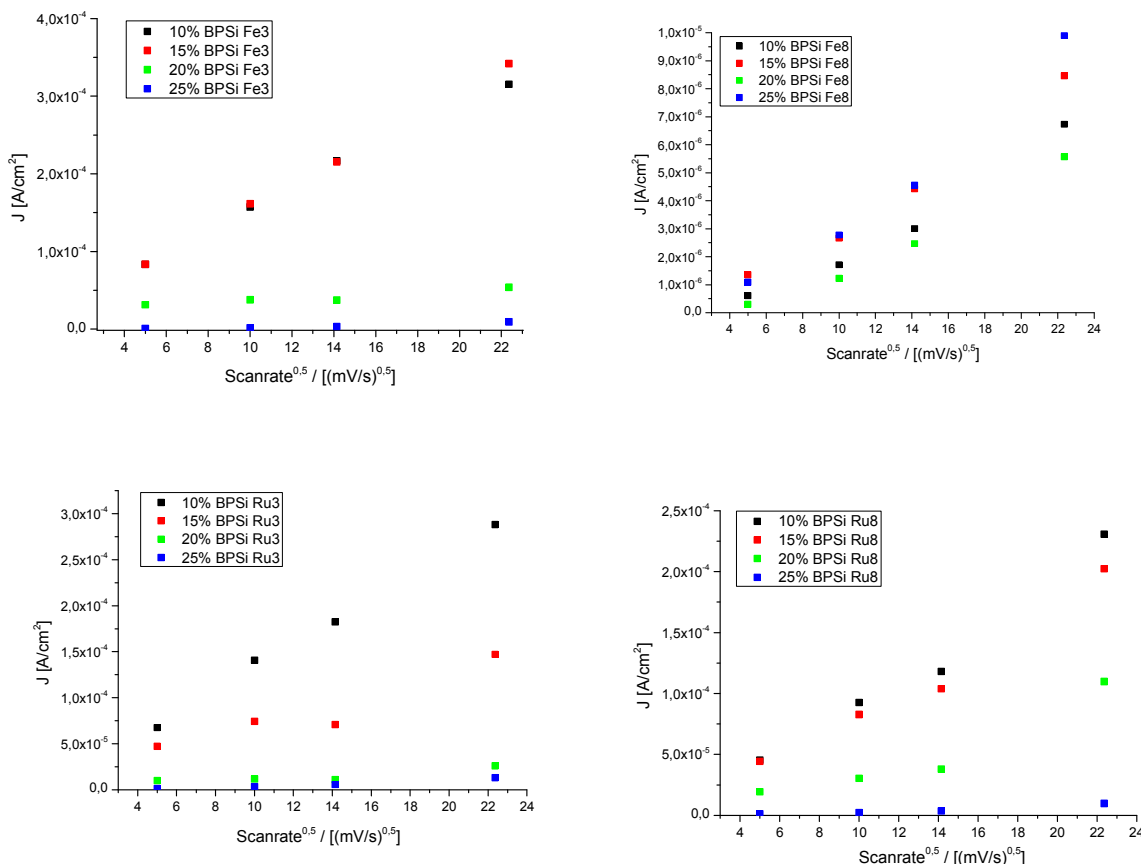


Figure S8. Cyclic voltammograms for NH₂Si mesoporous thin films with redox probe molecule $\text{Ru}(\text{NH}_3)_6^{3+}$ at pH ≤ 3 (a) and pH ≥ 8 (b) and the redox probe molecule $\text{Fe}(\text{CN})_6^{3-}$ at pH ≤ 3 (c) and pH ≥ 8 (d). The APTES ratio of 10 mol % is shown in black, 15 mol % in red, 20 mol % in green, and 25 mol % in blue.



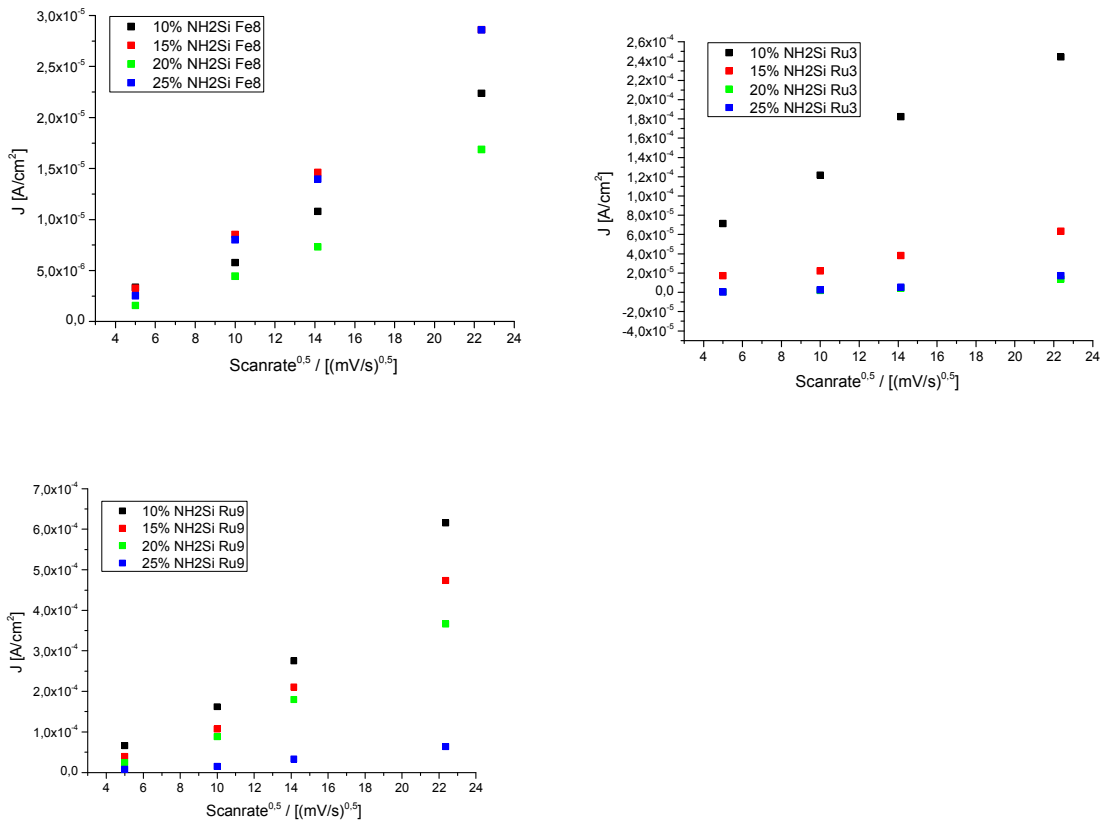


Figure S9. Maximum current density in dependence of the squareroot of the scanrate according to Randles-Sevcik equation for all mesoporous films. These data correspond to Figure 6, Figure S7 and Figure S8. A linear behavior is observed for all porous samples showing ionic accessibility of pores.

REFERENCES

1. Brunsen, A.; Calvo, A.; Williams, F. J.; Soler-Illia, G. J. A. A.; Azzaroni, O. Manipulation of Molecular Transport into Mesoporous Silica Thin Films by the Infiltration of Polyelectrolytes. *Langmuir* **2011**, *27*, 4328-4333.
2. Fontana, B. J. ; Thomas, J. R. The Configuration of Adsorbed Alkyl Methacrylate Polymers By Infrared and Sedimentation Studies. *J. Phys. Chem.* **1961**, *65*, 480-487.
3. Hess, C. ; Wild, U. ; Schlägl, R. The mechanism for the controlled synthesis of highly dispersed vanadia supported on silica SBA-15. *Microp. Mesop. Mater.* **2006**, *95*, 339-349.